Available online at www.sciencedirect.com
ScienceDirect
International Journal of Pharmaceutics 356 (2008) 110–120
INTERNATIONAL JOURNAL OF PHARMACEUTICS
www.elsevier.com/locate/ijpharm

Formulation, stability and thermal analysis of lyophilised wound healing wafers containing an insoluble MMP-3 inhibitor and a non-ionic surfactant

K.H. Matthews [a,*], H.N.E. Stevens [a], A.D. Auffret [b], M.J. Humphrey [b], G.M. Eccleston [a]

[a] *Department of Pharmaceutical Sciences, University of Strathclyde, Strathclyde Institute for Biomedical Sciences, 27 Taylor Street, Glasgow G4 ONR, UK*
[b] *Pfizer Central Research, Sandwich, Kent CT13 9NJ, UK*

Received 6 November 2007; accepted 31 December 2007
Available online 9 January 2008

Abstract

Lyophilised wafers are being developed as topical drug delivery systems for the treatment of chronic wounds. This study describes the formulation of xanthan wafers containing a selective, insoluble MMP-3 inhibitor (UK-370,106) and a non-ionic surfactant, designed to release accurate doses of UK-370,106 directly to a suppurating wound bed. Stability of UK-370,106 in the wafer compared to a non-lyophilised gel suspension was investigated using a combination of light scattering, thermal and microscopic techniques. Particle size distributions in UK-370,106-loaded wafers were constant throughout an accelerated stability study (12 weeks, 40 °C) while the mean particle size in a non-lyophilised suspension increased by 15 μm in the same period. Thermal analysis of UK-370,106-loaded wafers highlighted an unexpected interaction between the drug and the surfactant that was further investigated using simple mixtures of each component. It was concluded that an *in situ* solvate of UK-370,106 and the non-ionic surfactant can form and that this may have implications towards the stability of UK-370,106 during the formulation process. Further concerns regarding high water contents (14%) in the wafer and its effect on product stability were unfounded and it was concluded that these novel delivery systems provided a viable alternative to gel suspensions.

Keywords: Lyophilised wafer; Wound healing; UK-370,106; Surfactant; Stability; Thermal analysis

1. Introduction

Lyophilised wafers are produced by the freeze-drying of polymer solutions, suspensions and gels. They are designed to contain both soluble and insoluble therapeutic agents and be applied directly to the surface of suppurating wounds with minimum human contact. Formulation, production and rheological testing of lyophilised wound healing wafers have been described in detail (Matthews et al., 2003, 2005). The possibility of sterilising these novel dosage forms post-production using gamma-irradiation has also been investigated (Matthews et al., 2006) with promising results for wafers composed of xanthan gum. Such topical delivery systems offer many practical advantages over existing vehicles used for *in vivo* delivery of wound healing agents that include, polymer gels (Puolakkainen et al., 1995; Guzman-Gardearzabal et al., 2000), crosslinked hydrogels (Hubbell, 1996; Gombotz and Wee, 1998; Draye et al., 1998; Yamamoto et al., 2001; Masters et al., 2002; Obara et al., 2003; Cai et al., 2005; DeFail et al., 2006) and protein matrices (Ono et al., 1999; Gryzybowski et al., 1999; Sakiyama-Elbert and Hubbell, 2000; Yamaguchi and Yoshikawa, 2001).

A novel therapeutic agent for the selective inhibition of matrix metalloproteinase-3, stromelysin-1 (MMP-3), over-expressed in chronic dermal ulcers, is described in the literatures (Fray et al., 2001, 2003; Fray and Dickinson, 2001; Ashcroft et al., 2003) and available courtesy of Pfizer Ltd., UK. This particular member of the MMP family of zinc-centred enzymes is up-regulated in chronic (non-healing) dermal ulcers and thought to be responsible for proteolysis of fibronectin, a key compo-

* Corresponding author at: School of Pharmacy, The Robert Gordon University, Schoolhill, Aberdeen AB10 1FR, UK. Tel.: +44 1224 262546; fax: +44 1224 262555.
E-mail address: k.h.matthews@rgu.ac.uk (K.H. Matthews).

0378-5173/$ – see front matter © 2008 Elsevier B.V. All rights reserved.
doi:10.1016/j.ijpharm.2007.12.043

nent of 'provisional matrix'. This matrix consists of a mixture of collagen and fibronectin and acts as a scaffold for tissue reconstruction (Fray et al., 2003). Proteolysis of fibronectin is generally regarded as a key component of wound chronicity and fibronectin itself is known to be a good substrate for MMP-3 in particular. Other activated MMPs such as MMP-1, -2, -9 and -14 are also known to be conducive with normal wound healing (Saarialho-Kere et al., 1993; Salo et al., 1994; Takino et al., 1995) while MMP-13 is found deep in the chronic ulcer bed and thought to be associated with the remodelling of collagenous matrix (Vaalamo et al., 1997). A suitable therapeutic agent for improved healing of chronic wounds might then be expected to inhibit only MMPs-3 and -13 and have no inhibiting effect on MMPs-1, -2, -9 and -14. Selective control of MMPs should then change the physiological environment of chronic wound fluid to that of acute (healing) wounds.

The selective MMP-3 inhibitor UK-370,106 (Fig. 1), based on a derivative of succinyl hydroxamic acid, was initially tested by the oral dosing of rats (Fray et al., 2003) and high hepatic clearance and low bioavailability were apparent. Known side-effects associated with the ingestion of MMP inhibitors (Bird et al., 1998) and limited vascularisation in many chronic wounds, that prevented systemic compounds from reaching the wound site, further disfavoured oral dosing. For these reasons, and considering the importance of selectivity when using this compound, the authors opted for a topical delivery system.

The chosen vehicle for *in vivo* testing of UK-370,106 with a rat model involved topical application of the selective inhibitor as a "suspension in hydrogel" (Fray et al., 2003). Although it was concluded that the compound "was cleared rapidly from plasma, but slowly from dermal tissue", there was no indication of the quantity of agent lost to the wound environment via suppuration. This is not uncommon in topical studies due largely to the difficulty in controlling the precise quantity of therapeutic agent applied. The error is deemed to be highest when heavy degrees of suppuration are present and if a suppuration rate of >6 mL cm^{-2} in 24 h is considered 'moderate' (Thomas et al., 1996), presumably rates higher than this can be considered as 'heavy'. Based on observations from earlier model studies (Matthews et al., 2005) lyophilised wafers appeared to perform well in such a simulated environment.

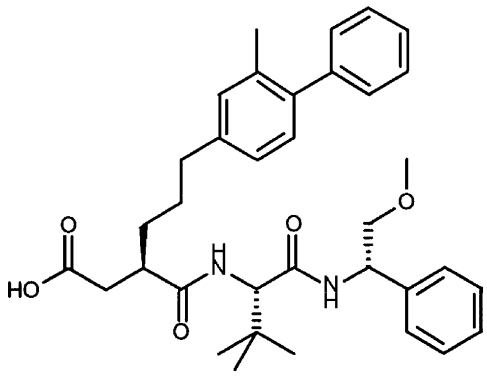

Fig. 1. Chemical structure of the drug, the selective MMP-3 inhibitor UK-370,106 (Fray et al., 2003).

Regarding the stability of UK-370,106 in a gel suspension, no studies appear to have been published, however, the crystalline structure has been characterised and several polymorphic forms are known to exist (Ashcroft et al., 2003). Single crystal X-ray data of a crystal of the drug grown from a non-aqueous solvent mixture indicated a planar structure containing large hydrophobic pockets in which the solvent was contained. These pores were thought to exist as "channels down the crystal framework" which could entrap the solvent molecules. Furthermore, gentle heating of these *in situ* solvates easily drove the entrapped solvent from the pores. This phenomenon was common for a variety of different solvents from which the compound had been crystallised. Most importantly, all solvates of the API essentially had the same planar structure, differing only in the size of the pores determined by the specific solvent or solvent combination. Lack of substantial hydrogen bonding between the crystal planes produced a degree of plasticity in the desolvated compounds which all had sharp melting points in the range 188–191 °C. The relatively recent concept of "channel solvates" as pseudopolymorphs (Skakle et al., 2001; Suitchmezian et al., 2006) would support these earlier conclusions.

In principle, the stability of polymorphic forms should be better in a lyophilised dosage form than a hydrogel suspension. In addition to offering a novel and 'fit for purpose' vehicle for the topical application of therapeutic reagents, the added advantage of encasement of the drug in a lyophilised matrix also offered the prospect of improved drug stability and extended shelf-life for a medicinal product thus formulated. It was anticipated that a lyophilised polymer matrix would preserve the size, shape and form of contained compounds unlike a conventional gel suspension, where crystal ripening (Mullin, 2001), agglomeration (Nichols et al., 2002) and polymorphic change may occur. Consequently, it was considered necessary to verify this conjecture. It was also assumed that the main effect of crystal ripening and/or agglomeration would be to increase the mean particle size of contained compounds.

To test this theory, an accelerated ageing study was undertaken on UK-370,106-loaded xanthan wafers and laser light scattering used to determine the particle size distribution of the drug as a function of ageing time. Non-aged wafers, containing increasing amounts of UK-370,106 were characterised using differential scanning calorimetry (DSC) and explanation of the results obtained was aided by a model DSC study consisting of the thermal analysis of simple combinations of UK-370,106 and surfactant. Thermogravimetric analysis (TGA) was used to measure the water content of wafers and dynamic vapour sorption (DVS) to investigate the relationship between relative humidity and water content for both drug-loaded and placebo xanthan wafers.

Optical microscopy was used for further qualitative analysis of UK-370,106 in the xanthan gel suspension and scanning electron microscopy (SEM) for analysis of the lyophilised wafers resulting from the mother suspension. Images obtained were used to support the other data generated.

This study is the first of its kind to describe the formulation, manufacture and stability testing of wafers containing a

therapeutic agent designed to improve the healing of chronic wounds.

2. Materials and methods

2.1. Materials

The MMP-3 inhibitor (3*R*)-3-({[(1*S*)-2,2-dimethyl-1-({[(1s)-2-methoxy-1-phenylethyl]amino}carbonyl)propyl]amino}-carbonyl)-6-(3-methyl-4-phenylphenyl) hexanoic acid (UK -370,106) (Fig. 1) was obtained from Pfizer Ltd., Sandwich, Kent, UK, as a highly water-insoluble, white crystalline compound. The water-soluble, non-ionic surfactant, Lutrol F68, used to aid suspension of UK-370,106 in deionised water, was obtained from Sigma–Aldrich, Gillingham, UK. Xanthan gum (Xantural^{TM}180) was obtained from CP Kelco US Inc., USA and used as received.

2.2. Production of wafers containing UK-370,106

Surfactant (0.12 g) was dissolved in deionised water (57.49 g) contained within a glass vial (100 ml) with manual agitation. UK-370,106 (1.80 g) was added and the mixture processed using a turbine mixer (Ultra Turrax T25 basic, IKA Labortechnik) fitted with a 8 mm head at its maximum speed of 24,000 rpm for 6 min. Xanthan gum (0.60 g) was then added as a dry powder and the vial stoppered and crimp-sealed. The vial was placed on a roller-mixer (Spiramix 10, Denley Instruments, Billinghurst, UK) overnight and a smoothly textured, white, homogeneous suspension of UK-370,106 in xanthan was obtained (Batch 1). The suspension was transferred to a large glass bottle (1000 mL) fitted with a stoppered valve and attached to a vacuum pump. Effective degassing of the gel suspension was achieved. The degassed suspension was cast (1.0 mL) using a syringe with a length of rubber tubing attached, to glass vials (5 mL, clear) and stoppered (20 mm, B2-40) prior to being freeze-dried. A placebo batch (Batch 2) containing no API was produced as a comparison (Table 1).

Degassed gel suspensions contained in semi-stoppered glass vials were placed in a chamber cooled, laboratory freeze-drier (*F.I.T. freeze drier*, *Serial No. SREC-00453*) and cooled to −25 °C over a period of 3 h followed by an isothermal primary drying stage for 24 h. The remainder of the cycle involved heating to +20 °C in 18 steps (equivalent to a heating rate of 2.5 °C/hr) giving a total cycle time of 45 h.

A further three batches (Batches 3–5) of xanthan wafers containing surfactant and three different quantities of UK-370,106 (1, 3 and 10 mg/mL or % (w/v) in the pre-lyophilised gel suspension) were similarly produced to investigate the effects of increased drug loadings on the wafers. This, in turn, led to an additional experiment to investigate the interaction between surfactant and UK-370,106 as discerned by DSC. A final batch of wafers containing 70 mg/ml (Batch 6) was also prepared to qualitatively assess the practical limits of insoluble drug loadings with this system and to determine the effect of high levels of hydrophobic drug on equilibrium moisture content (EMC) using TGA.

2.3. Accelerated stability

An accelerated stability trial was undertaken on the first two batches of wafers outlined in Table 1. Each batch of wafers was divided into two lots and one lot placed in a stability cabinet at 25 °C, the other being placed in a stability cabinet at the elevated temperature of 40 °C. Samples of the gel suspensions from which the wafers were produced (mother suspensions) were placed in air-tight, glass vials (2 mL) and stored at the higher temperature of 40 °C. These samples would provide a comparison for anticipated differences in the stability of UK-370,106 in both lyophilised and non-lyophilised gel suspensions.

2.4. Particle size analysis

Particle sizing of aged gel suspensions and wafers was undertaken using a magnetically stirred, small sample dispersion cell mounted within a *Malvern Mastersizer S* laser light scattering instrument. A 300 mm lens focussed the scattered beam ($\lambda = 633$ nm) onto a multi-diode detector. The detector consisted of an array of 48 light-sensitive diodes positioned to detect the scatter from particles measuring 0.6–878.7 μm. The total number of scans per measurement was 5000 and hence each distribution was the average of almost 250,000 individual readings. A curve displaying 'Abundance (%)' as a function of 'Particle Size' was displayed on the computer screen and the computed value for mean particle size was based on the statistics of polydisperse systems and used the volume mean diameter, $D[4, 3]$.

Table 1
Formulation details for six batches of xanthan wafers containing UK-370,106

Batch	UK-370,106		Lutrol F68		Xanthan gum		Water	
	(g)	(%, w/v)	(g)	(%, w/v)	(g)	(%, w/v)	(g)	(%, w/w)
1	1.80	3.00[a]	0.12	0.20[a]	0.60	1.00[a]	57.49	95.80
2	–	–	0.12	0.20[a]	0.60	1.00[a]	57.52	96.00
3	0.05	1	0.10	0.20	0.25	0.50	50.00[b]	–
4	0.15	3	0.10	0.20	0.25	0.50	50.00[b]	–
5	0.50	10	0.10	0.20	0.25	0.50	50.00[b]	–
6	3.50	70	0.10	0.20	0.25	0.50	50.00[b]	–

Batch 1 used in stability study. Weighing error ± 0.005 g.
[a] Equivalent concentration in pre-lyophilised gel (%, w/w).
[b] Volume (mL).

Filtered background solutions consisted of 0.2% (w/v) Lutrol F68 in deionised water. Although this concentration of surfactant is above the critical micelle concentration (Maskarinec et al., 2002) the presence of micelles does not interfere with the light scattering measurement as their average size is of the order of 10 nm (Alexandridis and Hatton, 1995) well below the minimum threshold for detection with this instrument.

Gel suspensions of UK-370,106 were administered directly to the dispersion cell. Wafers had to be reconstituted as their pre-lyophilised gels by the addition of deionised water (2 mL) with some intermittent, manual agitation for at least 1 h prior to measurement. A few seconds were allowed to ensure complete dispersion of the sample in the background solution before accumulating readings. It was apparent that all measurements were not static and were observed to drift to lower mean particle sizes as a function of time. To overcome this, all measurements were taken at 2-min intervals over a period of 10 min and the 'average mean' used. The results obtained are displayed in Table 2.

2.5. Microscopy

2.5.1. Optical microscopy

Subjective analysis of drug suspensions and lyophilised wafers using optical microscopy was conducted with a *Nikon AFX-II Labophot* optical microscope. Photographic images were recorded on *Polaroid* black and white film at different magnifications. Cross-polarising filters were available and used optionally. This technique was especially useful for assessing the nature of the drug suspensions in the gel formulations but not so useful with the 3D-structure of lyophilised wafers. A confocal microscope was also used to image wafers with little success.

2.5.2. Optical hot-stage microscopy

Attachment of a *Linkam THMSE 600* hot-stage with *TMS 92* temperature controller to the *AFX-II* optical microscope provided useful information on the phase changes detected in drug-loaded wafers and drug/surfactant mixtures. This information was used to corroborate some of the thermal events measured with DSC.

Table 2
Mean particle size and standard deviation for particles of UK-370,106 suspended in gels reconstituted from lyophilised wafers stored for varying periods at 25 and 40 °C

Batch no.	Mean particle size (±standard deviation) in microns			
	Storage (25 °C)		Storage (40°)	
	Time (weeks)	Wafer (μm)	Wafer (μm)	Gel suspension[a] (μm)
1	0	47.5 (±0.7)	47.5 (±0.7)	47.5 (±0.7)
	3	46.7 (±0.7)	47.2 (±1.2)	52.5 (±1.7)
	6	48.8 (±0.9)	46.2 (±1.3)	59.2 (±4.4)
	12	–	46.0 (±0.7)	62.0 (±0.5)

Samples of the original gel suspensions are also included following accelerated ageing at 40 °C.
[a] Mother suspensions were stored at 40 °C.

2.5.3. Scanning electron microscopy

An *Amray 1820 Scanning Electron Microscope* was used to image the structure of the drug-loaded wafers at the surface and in cross-section. Cross-sectional images were obtained by pulling the wafers apart orthogonally at 180° in opposite directions. Samples for imaging were gold sputtered for 3 min. Images reproduced result from laser scans of original prints produced using a video copy processor attached to the microscope.

2.6. Thermoanalytical methods

2.6.1. Differential scanning calorimetry

Following initial testing of lyophilised wafers using standard aluminium pans with crimped lids, wafer samples were manually compressed into large volume (60 μL), O-ring sealed, stainless steel sample pans (PerkinElmer Part No. 0319-0218/0319-00) to prevent the escape of significant quantities of water associated with the lyophilised matrix and improve the resolution of results (see Section 3.4). Placed on the sample stage of a *TA Instruments DSC2* with attached refrigerated cooling system, samples were initially cooled to −30 °C. After equilibration, heating to +75 °C was followed by a further period of cooling to −30 °C and a reheat to +350 °C.

For the analysis of simple ratios of surfactant to API, a single heating cycle from 25 to 250 °C at a heating rate of 5 °C/min was conducted.

2.6.2. Thermogravimetric analysis

The primary application of TGA was the determination of water contained in wafers. Samples were manually compressed to fit on the sample pan and heated from ambient temperature to 300 °C at 10 or 20 °C/min. A *TA Instruments Hi-Res TGA 2950* was used for all measurements.

2.6.3. Dynamic vapour sorption

The isothermal sorption and desorption of water as a function of relative humidity (%RH) was determined on a *Surface Measurement Systems Automated Water Sorption Analyser DVS-0*. Wafer samples were initially equilibrated at 0%RH and then at 15, 30, 45, 60, 75 and 90%RH and the weight gain (moisture sorption) measured. The process was then reversed in the same number of increments to 0%RH and the weight loss (moisture desorption) measured. A unique batch of drug-loaded wafers (Batch 6) containing the maximum amount of UK-370,106 that was practically possible (70 mg/mL) for a non-friable, solid dosage form, was used for DVS measurements. The drug content was equivalent to 6.50% (w/w) of UK-370,106 in the pre-lyophilised gel suspension, or a weight ratio of UK-370,106:xanthan of approximately 14:1 in the lyophilised wafer.

3. Results

3.1. Mean particle size of aged wafers and pre-lyophilised gel suspension

Reference to the mean particle sizes and standard deviations (Table 2) indicate no significant increase in the size of UK-

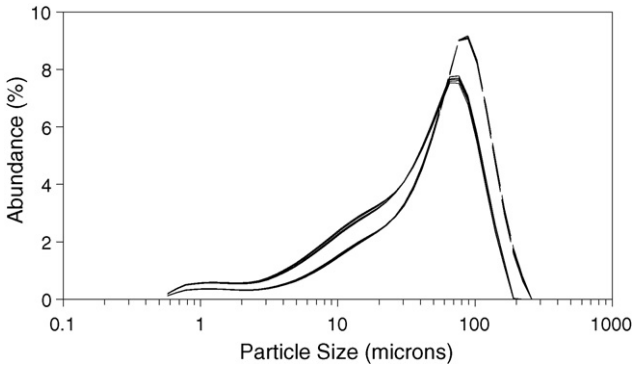

Fig. 2. Particle size distribution curves for UK-370,106-loaded wafers (—) (Batch 1) and the non-lyophilised gel suspension (mother suspension) (- - - -) aged for 12 weeks at 40 °C. A clear increase in the mean particle size is apparent for the mother suspension.

370,106 particles in aged wafer samples for Batch 1 at both 25 and 40 °C. This is in contrast to the notable and persistent increase in mean particle size of UK-370,106 in the mother suspension (stored at 40°). This increase, from 47.5 ± 0.7 μm at time 0 to 62.0 ± 0.5 μm at 12 weeks accelerated ageing, was in contrast to the maximum range of 46.7 ± 0.7–48.8 ± 0.9 μm for the aged wafers. The particle size distributions for both wafers and gel suspension are also presented (Fig. 2) and the unambiguous shift to a higher mean size of the disperse phase is apparent.

3.2. Optical microscopy of gel suspensions

Optical micrographs of the pre-lyophilised gel suspension (Batch 1) using transmitted light, indicated a very broad distribution of particle sizes under both brightfield (Fig. 3a) and cross-polarised conditions (Fig. 3b). The former image (100×) indicates a large variety of particle shapes, the largest, in the centre of the image, being in the 100–125 μm range (compare with Fig. 2). The bulk of the particles of UK-370,106 exist as either clusters (agglomerates) of smaller particles or *allotriomorphic* lumps. Some evidence of rhombic ('diamond-shaped') crystal geometries is barely visible at this magnification but at increased magnification (400×), planar rhombic forms are clearly visible (Fig. 4) and assumed to be single crystals of UK-370,106. The single crystal centred in the magnified image measures approximately 65 μm × 40 μm. Smaller single crystals are also visible around the centrepiece.

3.3. Scanning electron microscopy of UK-370,106-loaded wafers

The SEM images of a UK-370,106-loaded wafer from Batch 5 (Fig. 5a and b) are presented at two different magnifications. The lesser magnified image (Fig. 5a) shows a highly porous, sponge-like structure, typical of lyophilised polymer gels (McInnes et al., 2005). Greatly increased magnification (Fig. 5b) highlights crystals of UK-370,106 attached to the matrix structure. Details on the surface of the 35–60 μm particles highlighted were either part of the main crystal structures

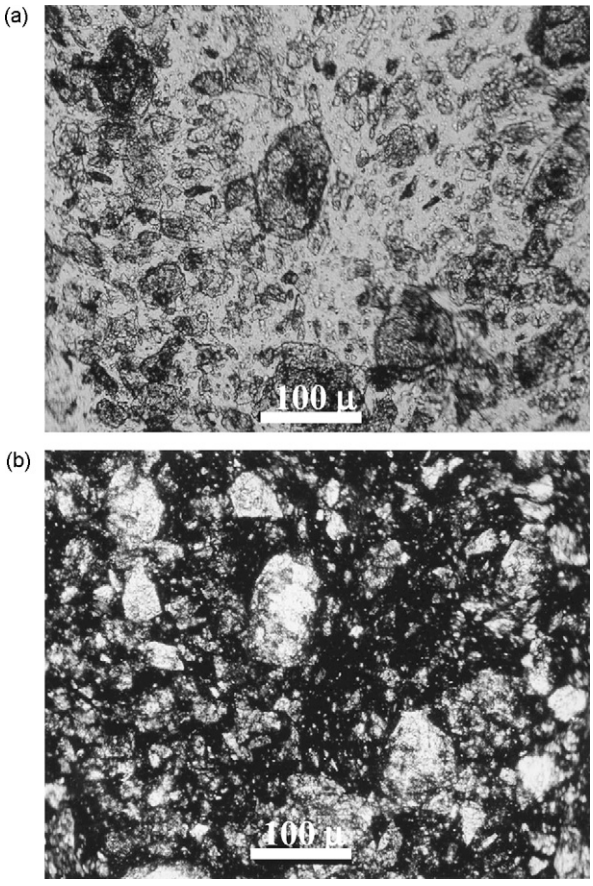

Fig. 3. Optical micrographs (magnification 100×) of a gel suspension containing UK-370,106 as an insoluble disperse phase and xanthan/water/Lutrol F68 as the continuous phase under conditions of brightfield (Fig. 3a) and between cross-polars (Fig. 3b). Note the large particle size distribution and highly crystalline nature of UK-370,106 in the suspension.

or smaller separate particles bound by lyophilised xanthan and formed during freeze-concentration.

3.4. Analysis of UK-370,106-loaded wafers by DSC

Initial testing of wafer samples using standard, sealed aluminium pans indicated a large, broad endotherm over the range

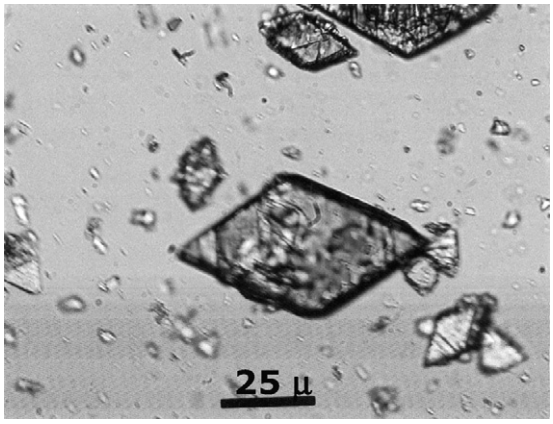

Fig. 4. Optical micrograph (magnification 400×) of single crystals of UK-370,106 of varying size from <10 to 50 μm in length. Note the planar rhombic symmetry.

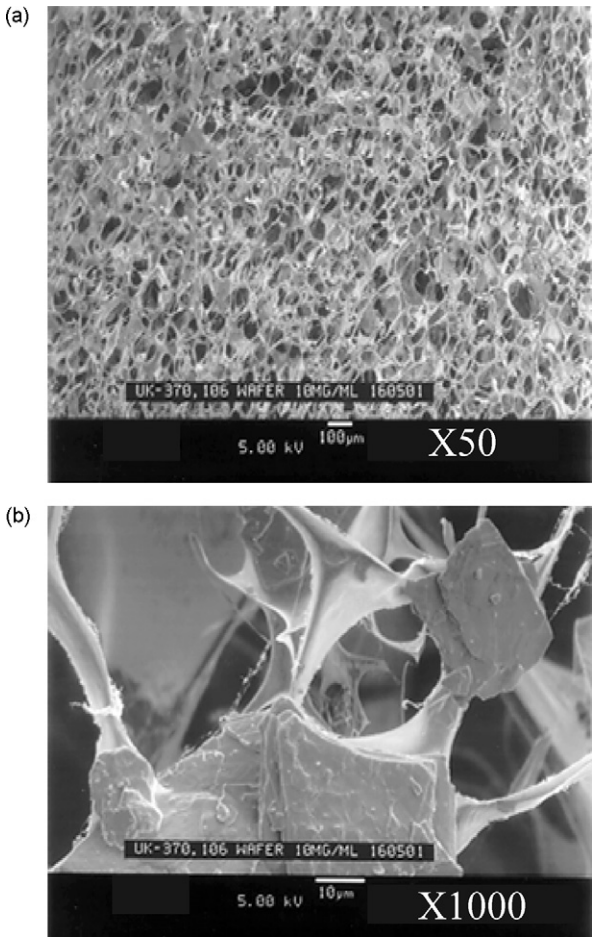

Fig. 5. SEM images of a UK-370,106-loaded wafer (Batch 5). The image at lower magnification (50×) (Fig. 5a) highlights the porous, 'sponge-like' morphology of lyophilised wafers. Higher magnification (1000×) (Fig. 5b) clearly shows crystals of UK-370,106 firmly attached to the porous matrix structure.

25–175 °C that was assumed to be due to loss of water from the hydrophilic matrices. The loss of significant quantities of moisture associated with wafers caused a constant change in the heat capacity, as a function of temperature, that accounted for the baseline deviation recorded. Continued analysis of wafers using hermetically sealed, large volume sample pans, contained the evaporative loss of water, eliminating the broad endothermic transition that threatened to minimise the chances of detecting weaker transitions in this temperature range (Fig. 6). Melting of the surfactant was clearly distinguishable and centred on 54 °C in the placebo xanthan wafers. Removal of the potentially obfuscating endotherm attributed to loss of water can also be seen to dramatically sharpen the large exotherm associated with the degradation of xanthan at around 250 °C and indicated a weak transition of undetermined origin at 160 °C.

Reference to the DSC results for Batches 2–5 (Fig. 7a and b) show the results obtained from the initial cool/heat/cool/heat cycle (+20 to −30 to +75 to −30 to +75 °C). This initial cycle (Fig. 7a) highlighted the fact that surfactant was present as an unreacted, solid crystalline component in the drug-loaded wafers as produced. Reasonably sharp melting, centred on 54.6 °C on the first heating cycle, was followed by recrystallisation below

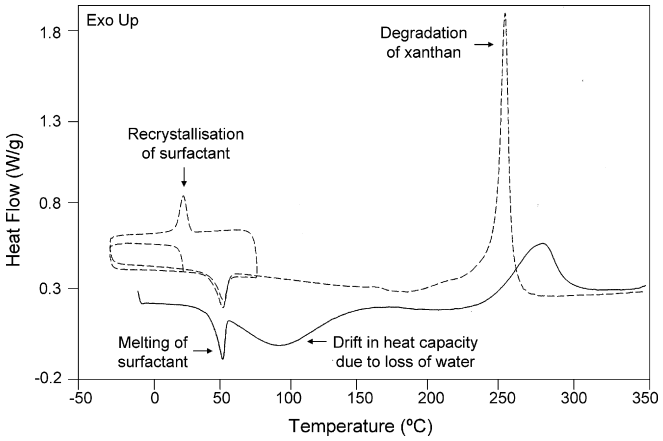

Fig. 6. DSC thermograms of placebo wafers (Batch 2) in standard aluminium (—) and large volume, stainless steel (- - - -) sample pans. Hermetic sealing in the latter pans suppresses the endothermic drift associated with water loss from the lyophilised wafer, levels the baseline and sharpens the exotherm associated with the degradation of xanthan. The cool/heat/re-cool/reheat cycle illustrated (20 to −30 °C/−30 to 75 °C/75 to −30 °C and −30 to 350 °C) shows the melting, recrystallisation and re-melting of the contained surfactant (Lutrol F68).

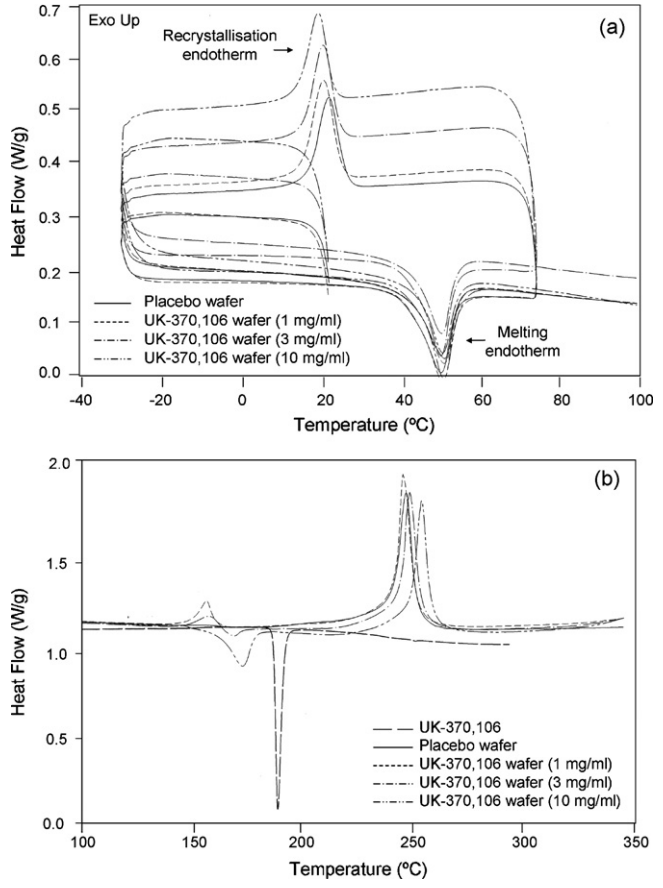

Fig. 7. DSC thermograms of the cool/reheat cycle (20 to −30 °C and −30 to 350 °C at 5 °C/min) for placebo (Batch 2) and UK-370,106-loaded wafers (Batches 3–5). Melting/recrystallisation/re-melting of the surfactant (Lutrol F68) (Fig. 7a) and interaction of molten surfactant and drug (Fig. 7b) are highlighted for xanthan wafers produced from gel suspensions containing 1, 3 and 10 mg/mL of UK-370,106. A sample of pure UK-370,106 (melting point 190 °C) is included for comparison.

+30 °C. On the second heating cycle, re-melting of the surfactant showed a small decrease in the enthalpy assumed to be indicative of a lower degree of crystallinity as a result of re-cooling. Continued heating to +350 °C (Fig. 7b) produced a complex series of exothermic and endothermic events in the 150–180 °C temperature range that were different for each UK-370,106-loaded wafer. Towards the end of the heating cycle, a large and sharply defined exotherm known to be associated with degradation of XG was also apparent. Each sample differed only in the amount of UK-370,106 contained (Table 1). Actual ratios of surfactant:UK-370,106 were 1:0 (placebo), 2:1, 2:3 and 1:5, respectively. Interestingly, it was noted that there was no pure melting endotherm at +190 °C for the free-acid form of UK-370,106 used. The free-acid form of UK-370,106 is superimposed for reference and centred on 190 °C (Fig. 7b). Clearly, the unexplained thermal behaviour for the three wafer samples analysed merited further investigation.

3.5. Application of DSC to UK-370,106—surfactant interactions

Analysis of simple mixtures of UK-370,106 and surfactant are presented (Fig. 8). When the amount of surfactant was in excess of UK-370,106 (UK-370,106:surfactant in weight ratio of 1:2) the most notable event was that of the melting of surfactant. This was followed by a gently sloping baseline that appeared to produce a weak endotherm over the 140–175 °C temperature range. This transition also appeared to have a double peak. Reversing the UK-370,106:surfactant weight ratio from 1:2 to 2:1 weakened the intensity of the surfactant melt transition and levelled the baseline to 140 °C. Subsequently, a clear and sharply defined exothermic transition, peak value 156.6 °C, was followed by an equally pronounced endotherm with peak value 175.0°. This pattern was repeated at the increased weight ratio of UK-370,106:surfactant, 4:1, but with shifts to higher temperature for both events of 161.7 and 183.3 °C, respectively. Finally the maximum weight ratio of UK-370,106:surfactant of 5:1, appeared to exhibit a single endothermic transition centred

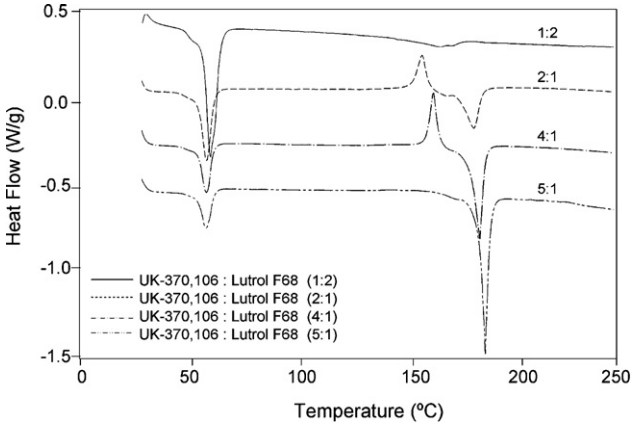

Fig. 8. DSC thermograms (single heat cycle from 25 to 250 °C at 5 °C/min) for four different mass ratios of UK-370,106:surfactant. Note the appearance (2:1) and disappearance (5:1) of the exotherm thought to be associated with the formation of solvate.

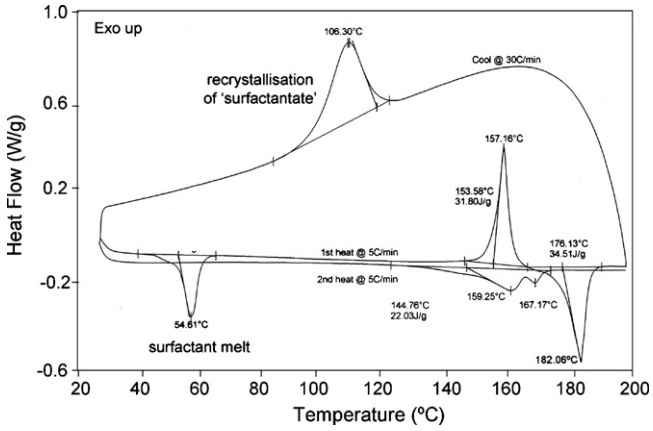

Fig. 9. DSC thermogram (heat/cool/reheat) of a UK-370,106-loaded wafer containing the maximum loading of UK-370,106 for a non-friable wafer (25–200 °C at 5 °C/min; 200–25 °C at 30 °C/min and 25–200 °C at 5 °C/min). Note the disappearance of the endotherm associated with melting of surfactant at 54.6 °C and the strong exotherm thought to be associated with the formation (onset 159.2 °C) and melting (onset 176.1 °C) of solvate.

on 185.6 °C, more than 4° lower than the pure compound as received.

Similarities between the results of DSC analysis of these mixtures with those of the UK-370,106-loaded wafers (Fig. 7b) were noted.

A further analysis of the 4:1 mixture was undertaken using a heat/cool/reheat cycle to further investigate the proposed interaction between UK-370,106 and surfactant (Fig. 9). Initial heating indicated the melting of surfactant, onset 50.6 °C, centred on 54.6 °C and showing an enthalpy equivalent to +20.8 J/g. A reasonably stable baseline gave way to a strong exotherm, −31.8 J/g, onset 153.6 °C, peak 157.2 °C. Immediately following this event, an inflection to an equally strong endothermic transition, onset 176.1 °C, peaking at 182.1 °C, suggested the melting of a compound that had just recrystallised. Cooling of the sample supported this conclusion as approximately one-third of the enthalpy of melting was retrieved by a further recrystallisation peaking at 106.3 °C. At the start of the second heating cycle, the apparent absence of the melting endotherm for the surfactant confirmed that the recrystallisation observed on the cooling curve must be the result of some combination, reaction or complex between UK-370,106 and surfactant that had formed on the initial heating cycle. Continued heating produced a broad onset starting around 130 °C and calculated at 144.8 °C that appeared to have two clear maxima at 159.2 and 167.2 °C, with a combined enthalpy of +22.0 J/g. The strong endothermic transition at 182.1 °C, apparent on the first heating cycle, was absent.

3.6. Determination of water content by TGA

TGA analysis was successfully used to determine the total water content of lyophilised wafers. The weight loss measured between ambient and 175 °C reflected the total water content of the sample. Further weight losses were associated with degradation of the sample and of no great interest to these studies.

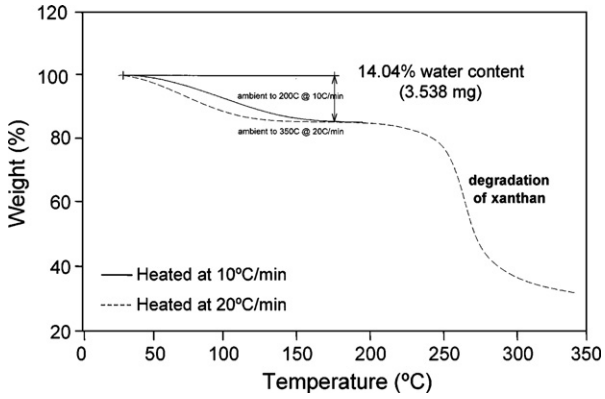

Fig. 10. TGA thermograms for the placebo wafer (Batch 2) indicating a weight loss equivalent to 14.04% (w/w) in the ambient to 200 °C range associated with water content of the lyophilised wafer. The subsequent and larger weight loss is associated with degradation of xanthan and of no particular interest to these studies.

A typical result is exemplified (Fig. 10) for the placebo wafer (Batch 2). Irrespective of the heating rates of 10 or 20 °C/min, water content was measured at 14.04% (w/w) for this particular sample. It should be noted that this result is for illustrative purposes and that the equilibrium moisture content of wafers will reflect environmental conditions.

3.7. Dynamic vapour sorption

The sorption/desorption properties of both UK-370,106-loaded and -unloaded wafers are represented as a function of relative humidity (%RH) at 30 °C (Fig. 11). The placebo wafer absorbed 47.3% of its weight in water between 0 and 90%RH. A drug-loaded wafer containing the maximum amount of UK-370,106 that was practically feasible for a xanthan wafer (70 mg UK-370,106 per mL of pre-lyophilised gel) produced values for water content that were one-quarter that of the placebo. It

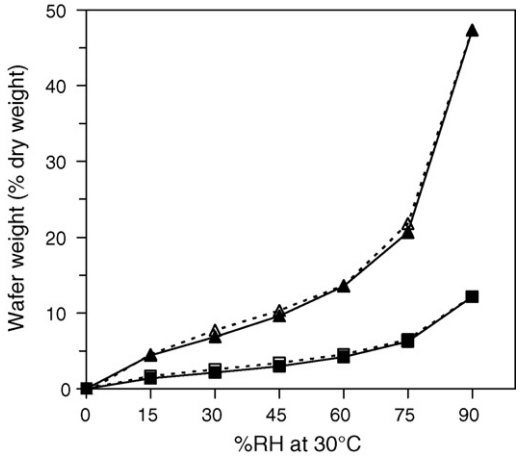

Fig. 11. Sorption/desorption isotherms for placebo ((▲) sorption/(△) desorption) (Batch 2) and API-loaded ((■) sorption/(□) desorption) (Batch 6) wafers as determined by DVS. The relative humidity was varied from 0 to 90%RH and 90–0%RH at 30 °C. High loading of the hydrophobic drug effectively reduces the hydrophilicity of the lyophilised matrix.

appeared that the API-loaded wafers were less prone to absorb water than the placebo wafers.

4. Discussion

Accelerated stability of UK-370,106-loaded wafers (Batch 1) confirmed that there was no significant change to the mean particle size or particle size distribution at both storage temperatures (Table 1). It was thus concluded that the freeze-drying process had no effect on the particle size of this 'insoluble' drug, nor did storage at 40 °C for 12 weeks. This was in contrast to the clear and significant change in the mean particle size of a similarly aged gel suspension of UK-370,106 (Table 2 and Fig. 2). The reasons for the increased particle size in the non-lyophilised suspension were not conclusive and could be attributed either to Ostwald ripening (Mullin, 2001), the formation of bound assemblages of drug particles ('hard' and 'soft agglomerates' as suggested by Nichols et al., 2002 in relation to powders) or a combination of both phenomena. In colloid science, flocculation, coalescence and coagulation also describe different states of particle assemblage and could arguably be used to explain the increased size of UK-370,106 particles in the aged gel suspension. However, due to the uncharged nature of UK-370,106, the terminology from powder technology was chosen.

From consideration of optical micrographs of the gel suspension (Fig. 3a and b) the larger particles of UK-370,106 appeared to be composed of agglomerations of smaller crystalline particles that were dispersed to varying degrees by the application of a cover slip during sample preparation. According to Nichols et al. (2002), hard agglomerates are not dispersed under such external shearing forces whereas soft agglomerates are, liberating primary crystalline particles. It was concluded that UK-370,106 in these suspensions is composed of a mixture of hard and soft agglomerates.

A high degree of crystallinity for the API can be inferred from the strong birefringence apparent under cross-polarised conditions (Fig. 3b). Closer examination of primary particles at higher magnification (Fig. 4) indicated a planar rhombic geometry typical of single crystals. The appearance of very small rhombic particles (<10 μm) alongside much larger crystals (>50 μm) would appear to be conducive with the conditions required for Ostwald ripening, where the smallest crystals dissolve in the continuous phase only to recrystallise as part of the larger crystals of the disperse phase. The nature of the crystalline dispersion at the point of freeze-concentration was clearly maintained throughout the lyophilisation process, as can be inferred from the SEM image presented (Fig. 5b). The image at lower magnification (Fig. 5a) confirms the highly porous structure of lyophilised polymer matrices.

Further investigations of the nature of UK-370,106 contained in the lyophilised xanthan matrix were commenced using DSC. Once the problem of large drifts in the heat capacity, due to water loss from the wafers, was addressed by using large volume, hermetically sealed, stainless steel sample pans (Fig. 6); all wafer samples showed relatively large endotherms, attributed to the melting of solid surfactant (Lutrol F68). This non-ionic surfactant was used during the formulation procedure to aid dis-

persion and suspension of the highly hydrophobic UK-370,106 in distilled water prior to the addition of xanthan gum. Clearly, solubilised surfactant had re-crystallised during the freezing cycle of the lyophilisation process, separating as a solid phase in the freeze-concentrated formulation. Upon initial heating of wafer samples, the melting was readily detected at 54.6 °C. Subsequent cooling from 75 to −25 °C caused the surfactant to re-crystallise with a slightly reduced degree of crystallinity, as evidenced by a decreased enthalpy of melting upon subsequent heating (Fig. 7a). This behaviour was the same for both UK-370,106-loaded and placebo wafers, confirming that Lutrol F68 was present as a separate phase, with no apparent effect on the mechanical properties of the wafers as subjectively assessed.

Subsequent heating of the wafers in the presence of molten surfactant, however, had a profound effect on the thermal behaviour measured in the 150–180 °C temperature range. It appeared that following the melting of surfactant to an isotropic liquid, as evidenced by hot-stage microscopy, crystalline particles of UK-370,106 appeared to begin to dissolve and re-crystallise simultaneously in the liquid phase at 150 °C. This observed phase change/s corresponded with the onset of a significant exothermic transition in the DSC results for two of the five samples displayed (Fig. 7b), namely the loaded wafers containing 1 and 3 mg/mL of UK-370,106 (based on the pre-lyophilised gel suspensions) or weight ratios of UK-370,106 to surfactant of 1:2 (Batch 3) and 3:2 (Batch 4), respectively. The placebo wafer (Batch 2) showed no notable transition while the 10 mg/mL wafer (Batch 5) containing a ratio of UK-370,106 to surfactant of 5:1, displayed only an endothermic transition centred on 185.6 °C. The appearance of a crystalline melt transition for the pure form of UK-370,106 in the range of 188–191 °C, was notable by its absence. The melt transition for the pure sample of UK-370,106 used in this study is shown for reference purposes and centred on 190 °C (Fig. 7b). It was clear that UK-370,106 was interacting with the molten surfactant above 150 °C.

Based on the knowledge that UK-370,106 was able to form *in situ* solvates with solvents such as acetone and cyclohexanone (Ashcroft et al., 2003), it seemed feasible that liquid surfactant may also act like a solvent and form *in situ* solvates, or channel solvates, desolvation of which would be relatively slow due to the non-volatile nature of the surfactant. It can be reasoned that long and flexible poly(ethyleneoxy)/poly(propyleneoxy) molecules of Lutrol F68 are able to 'wriggle' into the pores formed by hydrogen-bonded slip-planes and remain there indefinitely. The evidence of hot-stage microscopy and DSC analysis of UK-370,106-loaded wafers containing Lutrol F68, presented in this study, would support this hypothesis for the formation of such solvates during thermal analyses. Of course, formation of solvates requires direct contact between the solid drug and a mobile liquid containing the surfactant. In a lyophilised wafer at room temperature, such a mobile liquid phase does not exist and so no interaction can, in principle, take place. However, this would not be the case in the gel suspension where the surfactant is dissolved in water and therefore free to migrate into the pores of insoluble UK-370,106. Consequently for the wafer technology, formation of the solvate might be expected to occur at the formulation stage prior to lyophilisation but no direct evidence of this was available as no X-ray diffraction studies have been undertaken on drug-loaded wafers.

This probable interaction between UK-370,106 and Lutrol F68 was investigated further using simple mixtures of both the drug and surfactant. It was not fully understood if the strong exotherms detected in the 2:1 and 4:1 (UK-370,106:surfactant) mixtures, at 156.6 and 161.7 °C, were due to re-crystallisation of the solvate prior to melting at 175.0 and 183.3 °C, respectively or simple dissolution of some UK-370,106 in molten surfactant (exothermic) followed closely by melting of effectively 'impure' UK-370,106.

Co-existence of solvate with pure UK-370,106 (or desolvated UK-370,106) may even be considered a co-crystal in terms of the co-existence of two similar (but non-identical) crystalline forms of UK-370,106 (Desiraju, 2003). More simply, co-existence of the solvate with the desolvate may be expected to produce a depression in the melting point of the desolvate, which was known to be 190 °C (Fig. 7b). However, the relative intensity of the exotherms detected by DSC at ratios of 2:1 and 4:1 (Fig. 8) taken in conjunction with evidence of a dissolution/re-crystallisation event at around 150 °C (hot-stage microscopy) suggested formation of a crystalline solvate. The subsequent melting endotherm of the solvate was then possibly affected by the relative amounts of desolvated UK-370,106. In the sample with weight ratio 1:2, the solvate cannot crystallise in an excess of molten surfactant hence the absence of the exotherm and relative weakness of the subsequent endotherm. In the 5:1 mixture, the solvate cannot crystallise as there is an insufficient amount formed.

Evidence from the final DSC presented (Fig. 9) confirms that the surfactant was unable to crystallise in its pure form following the formation of solvate. During the second heating cycle, a broad endotherm with two clear maxima was apparent and possibly indicative of the co-existence of solvate and desolvate, the known melting point of the desolvate (190°) being depressed by the presence of solvate, *i.e.* a eutectic melt. The absence of a strong exotherm on the second heating cycle was also symptomatic of all the surfactant being already included within the crystal structure of UK-370,106 but the solvate being unable to recrystallise in a truly pure form due to the presence of desolvate.

The interaction of UK-370,106 and surfactant was clearly complex and such considerations as those discussed were only relevant in terms of understanding the thermal behaviour of UK-370,106-loaded wafers above normal working temperatures, or the probability of solvate formation during the formulation process. More relevantly, the levels of residual water from the freeze-drying process and/or the EMC of the lyophilised wafers may be of more concern with regards to the stability of these novel solid dosage forms. To these ends, TGA was used to determine the water content of wafer samples while DVS was used to define the moisture sorption/desorption properties.

Placebo wafer samples, highlighted (Fig. 10), appeared to have a water content of 14.04% (w/w) by TGA, the two heating rates used (10 and 20 °C/min) giving exactly the same result. At first sight, it seems infeasible that an apparently sta-

ble lyophilised product should have such a relatively high water content and still retain its shape as cast prior to lyophilisation. It should be borne in mind that the glass transition temperature (T_g) of the lyophilised polymer matrix must be above room temperature, even at the EMC of the polymer from which the matrix is constructed. EMCs for carbohydrates and cellulose ethers are typically in the 10–20% (w/w) range under normal atmospheric conditions (Kibbe, 2000). Other experimental work undertaken during the course of these studies (not shown) has highlighted the fact that, following thorough removal of non-freezing water in the final stages of a freeze-drying cycle to produce wafers, low water contents of <3% (w/w) are readily obtainable but are quickly increased by fast equilibration to normal laboratory atmospheric conditions. Providing the depression of the T_g of the glassy polymer matrix, by increased water content, does not fall below the operational or storage temperature of the wafer, the shape will remain intact for an indefinite period. In our laboratories, wafer samples stored in 'dry' but uncontrolled environments for more than 7 years are still intact.

The ease with which moisture is absorbed and desorbed is highlighted by the superimposition of both sorption and desorption curves for the placebo and drug-loaded samples as a function of relative humidity (Fig. 11). Water content at 90%RH is 47.3% (w/w) for the placebo wafer and 12.2% (w/w) for the UK-370,106-loaded sample. The inherently hydrophobic nature of UK-370,106 and its high concentration in the xanthan wafer tested has effectively made the dosage form less hydrophilic. Lower quantities of water in the lyophilised matrix of the UK-370,106-loaded wafer will limit the depression of T_g compared to placebo wafers resulting in a relatively more stable product. Re-examination of the scanning electron microscopy image illustrate the distinct solid phases of both UK-370,106 and the glassy matrix (Fig. 5b), the former phase appearing tightly bound to the supporting network structure. Assuming that the surfactant resides predominantly in the latter phase, based on DSC results of as-made wafers and the appearance of Lutrol F68 as a crystalline compound within the dosage form, solvate formation within UK-370,106-loaded wafers is highly unlikely below the T_g of the lyophilised structure. Diffusional processes within glassy polymers are extremely slow due to lack of translational motion within the molecular structure but could, in principle, be measured by X-ray diffractional methods over time.

It is clear that lyophilised wafers can provide a stable and effective storage medium for insoluble therapeutic agents designed to be delivered directly (topically) to the site of action. The release of contained therapeutic agents will be governed by the choice of polymer and the rheological characteristics of the gel state *in situ* (Matthews et al., 2005), which will in turn be influenced by the degree of suppuration from the chronic wound bed. The uptake of therapeutic agent and its concentration and residence in the wound bed will then become the critical factors governing the efficacy of this novel and interesting dosage form. Although this work details a specific MMP-3 inhibitor and its incorporation in a lyophilised xanthan wafer, the formulation method and characterisation techniques described to investigate the stability of UK-370,106 could be universally applied to a wide variety of therapeutic agents.

Acknowledgements

The authors wish to thank Pfizer Ltd., UK, for the funding with which these studies were possible and Dr. Gary Nicols (Pfizer Ltd., UK) for producing the SEM images.

References

Alexandridis, P., Hatton, T.A., 1995. Poly(ethylene oxide)-poly(propylene oxide)-poly(ethylene oxide) block copolymer surfactants in aqueous solutions and at interfaces: thermodynamics, structure, dynamics, and modelling. Colloid Surf. A: Physicochem. Eng. Aspects 96, 1–46.

Ashcroft, C.P., Challenger, S., Derrick, A.M., Storey, R., Thomson, N.M., 2003. Asymmetric synthesis of an MMP-3 inhibitor incorporating a 2-alkyl succinate motif. Org. Process Res. Dev. 7, 362–368.

Bird, J., Montana, J.G., Wills, R.E., Baxter, A.D., Owen, D.A., 1998. Selective MMP-3 inhibitors having reduced side-effects. International Patent. Darwin Discovery Ltd., WO 9,839,024, November 09.

Cai, S.S., Liu, Y.C., Shu, X.Z., Prestwich, G.D., 2005. Injectable glycosaminoglycan hydrogels for controlled release of human basic fibroblast growth factor. Biomaterials 26, 6054–6067.

DeFail, A.J., Chu, C.R., Izzo, N., Marra, K.G., 2006. Controlled release of bioactive TGF-beta(1) from microspheres embedded within biodegradable hydrogels. Biomaterials 27, 1579–1585.

Desiraju, G.R., 2003. Crystal or co-crystal. Cryst. Eng. Commun. 5, 466–467.

Draye, J.P., Delaey, B., Van de Voorde, A., Van den Bulcke, A., Bogdanov, B., Schacht, E., 1998. In vitro release characteristics of bioactive molecules from dextran dialdehyde cross-linked hydrogel films. Biomaterials 19, 99–107.

Fray, M.J., Dickinson, R.P., 2001. Discovery of potent and selective succinyl hydroxamate inhibitors of matrix metalloproteinase-3 (stromelysin-1). Bioorg. Med. Chem. Lett. 11, 571–574.

Fray, M.J., Burslem, M.F., Dickinson, R.P., 2001. Selectivity of inhibition of matrix metalloproteinase MMP-3 and MMP-2 by succinyl hydroxamates and their carboxylic acid analogues is dependent on P3′ group chirality. Bioorg. Med. Chem. Lett. 11, 567–570.

Fray, M.J., Dickinson, R.P., Huggins, J.P., Occleston, N.L., 2003. A potent, selective inhibitor of matrix metalloproteinase-3 for the topical treatment of chronic dermal ulcers. J. Med. Chem. 46, 3514–3525.

Gombotz, W.R., Wee, S.F., 1998. Protein release from alginate matrices. Adv. Drug. Deliv. Rev. 31, 267–285.

Gryzybowski, J., Oldak, E., Antos-Bielska, M., Janiak, M.K., Pojda, Z., 1999. New cytokine dressing. I. Kinetics of the in vitro rhG-CSF, rhGM-CSF and rhEGF release from the dressings. Int. J. Pharm. 184, 173–178.

Guzman-Gardearzabal, E., Leyva-Bohorquez, G., Sala-Coiln, S., Paz-Janeiro, J.L., Alvarado-Ruiz, R., Garcia-Salazar, R., 2000. Treatment of chronic ulcers in the lower extremeties with topical becaplermin gel 0.01%: a multicenter open-label study. Adv. Ther. 17, 184–189.

Hubbell, J.A., 1996. Hydrogel systems for barriers and local drug delivery in the control of woundhealing. J. Contr. Release 39, 305–313.

Kibbe, A.H., 2000. Handbook of Pharmaceutical Excipients, 3rd ed. Pharmaceutical Press, London.

Maskarinec, S.A., Hannig, J., Lee, R.C., Lee, K.Y.C., 2002. Direct observation of Poloxamer 188 insertion into lipid monolayers. Biophys. J. 82, 1453–1459.

Masters, K.S.B., Leibovich, S.J., Belem, P., West, J.L., Poole-Warren, L.A., 2002. Effects of nitric oxide releasing poly(vinyl alcohol) hydrogel dressings on dermal wound healing in diabetic mice. Wound Repair Regen. 10, 286–294.

Matthews, K.H., Stevens, H.N.E., Auffret, A.D., Humphrey, M.J., Eccleston, G.M., 2003. Wafer for wounds. International Patent. Pfizer Ltd., WO 03,037,395, August 05.

Matthews, K.H., Stevens, H.N.E., Auffret, A.D., Humphrey, M.J., Eccleston, G.M., 2005. Lyophilised wafers as a drug delivery system for wound healing containing methylcellulose as a viscosity modifier. Int. J. Pharm. 289, 51–62.

Matthews, K.H., Stevens, H.N.E., Auffret, A.D., Humphrey, M.J., Eccleston, G.M., 2006. Gamma-irradiation of lyophilised wound healing wafers. Int. J. Pharm. 313, 78–86.

McInnes, F.J., Thapa, P., Baillie, A.J., Welling, P.G., Watson, D.G., Gibson, I., Nolan, A., Stevens, H.N.E., 2005. In vivo evaluation of nicotine lyophilised nasal insert in sheep. Int. J. Pharm. 304, 72–82.

Mullin, J.W., 2001. Crystallisation, 4th ed. Elsevier.

Nichols, G., Byard, S., Bloxham, M.J., Botterill, J., Dawson, N.J., Dennis, A., Diart, A., North, N.C., Sherwood, J.D., 2002. A review of the terms agglomerate and aggregate with a recommendation for nomenclature used in powder and particle characterisation. J. Pharm. Sci. 91, 2103–2109.

Obara, K., Ishihara, M., Ishizuka, T., Fujita, M., Ozeki, Y., Maehara, T., Saito, Y., Yura, H., Matsui, T., Hattori, H., Kikuchi, M., Kurita, A., 2003. Photocrosslinkable chitosan hydrogel containing fibroblast growth factor-2 stimulates wound healing in healing-impaired db/db mice. Biomaterials 24, 3437–3444.

Ono, I., Tateshita, T., Iniue, M., 1999. Effects of collagen matrix containing basic fibroblast growth factor on wound contraction. J. Biomed. Mater. Res. 48, 621–630.

Puolakkainen, P.A., Twardzik, D.R., Ranchalis, J.E., 1995. The enhancement in wound healing by transforming growth factor-beta (1) (TGF-beta(1)) depends on the topical delivery system. J. Surg. Res. 58, 321–329.

Saarialho-Kere, U.K., Kovacs, S.O., Pentland, A.P., 1993. Cell matrix interaction modulated interstitial collagenase expression by human keratinocytes actively involved in wound healing. J. Clin. Invest. 92, 2858–2866.

Sakiyama-Elbert, S.E., Hubbell, J.A., 2000. Controlled release of nerve growth factors from a heparin-containing fibrin-based cell ingrowth matrix. J. Control Release 69, 149–158.

Salo, T., Makanen, M., Kylmaniemi, M., Autio-Harmainen, H., Larjava, H., 1994. Expression of matrix metalloproteinase-2 and -9 during early human wound healing. Lab. Invest. 70, 176–182.

Skakle, J.M.S., Wardle, J.L., Low, J.N., Glidewell, C., 2001. Solvated and solvent-free forms of *N*,*N*′-dithiodiphthalimide. Acta Cryst. C57, 724–746.

Suitchmezian, V., Jess, I., Nather, C., 2006. Crystal structures and properties of two new pseudopolymorphic modifications of the glucocorticoide triamcinolone diacetate. Solid State Sci. 8, 1373–1379.

Takino, T., Sato, H., Shinagawa, A., Seiki, M., 1995. Identification of the second membrane-type matrix metalloproteinase (MT-MMP-2) gene from a human placenta cDNA library. MT-MMPs form a unique membrane-type subclass in the MMP family. J. Biol. Chem. 270, 23013–23020.

Thomas, S., Fear, M., Humphreys, J., Disley, L., Waring, M.J., 1996. The effects of dressings on the production of exudates from venous leg ulcers. Wounds 8, 145–149.

Vaalamo, M., Mattila, L., Johansson, N., Kariniemi, A.L., Karjalainen-Lindsberg, M.L., Kahari, V.M., Saarialho-Kere, U.K., 1997. Distinct populations of stromal cells express collagenase-3 (MMP-13) and collagenase-1 (MMP-1) in chroninc ulcers but not in normally healing wounds. J. Invest. Dermatol. 109, 96–101.

Yamaguchi, Y., Yoshikawa, K., 2001. Cutaneous wound healing—an update. J. Dermatol. 28, 521–534.

Yamamoto, M., Ikada, Y., Tabata, Y., 2001. Controlled release of growth factors based on biodegradation of gelatin hydrogel. J. Biomater. Sci.-Polym. Ed. 12, 77–88.